G. V. Nikiforovich[1,2]
S. D. Sharma[1]
M. E. Hadley[3]
V. J. Hruby[1]
[1] *Department of Chemistry, University of Arizona, Tucson, AZ 85721*

[2] *Center for Molecular Design, Washington University, St. Louis, MO 63110*

[3] *Department of Anatomy, University of Arizona, Tucson, AZ 85721*

Received 7 February 1997; accepted 25 February 1998

Studies of Conformational Isomerism in α-Melanocyte Stimulating Hormone by Design of Cyclic Analogues

Abstract: *Results of energy calculations for α-MSH (α-melanocyte stimulating hormone, Ac-Ser[1]-Tyr[2]-Ser[3]-Met[4]-Glu[5]-His[6]-Phe[7]-Arg[8]-Trp[9]-Gly[10]-Lys[11]-Pro[12]-Val[13]-NH_2) and [D-Phe[7]]α-MSH were used for design of cyclic peptides with the general aim to stabilize different conformational isomers of the parent compound. The minimal structural modifications of the conformationally flexible Gly[10] residue, as substitutions for L-Ala, D-Ala, or Aib (replacing of hydrogen atoms by methyl groups), were applied to obtain octa- and heptapeptide analogues of α-MSH(4–11) and α-MSH(5–11), which were cyclized by lactam bridges between the side chains in positions 5 and 11. Some of these analogues, namely those with substitutions of the Gly[10] residue with L-Ala or Aib, showed biological activity potencies on frog skin comparable to the potency of the parent tridecapeptide hormone. Additional energy calculations for designed cyclic analogues were used for further refinement of the model for the biologically active conformations of the His-Phe-Arg-Trp ''message'' sequence within the sequences of α-MSH and [D-Phe[7]]α-MSH. In such conformations the aromatic moieties of the side chains of the His[6], L/D-Phe[7], and Trp[9] residues form a continuous hydrophobic ''surface,'' presumably interacting with a complementary receptor site. This feature is characteristic for low-energy conformers of active cyclic analogues, but it is absent in the case of inactive analogues. This particular spatial arrangement of functional groups involved in the message sequence is very close for α-MSH and [D-Phe[7]]α-MSH, as well as for biologically active cyclic analogues despite differences of dihedral angle values for corresponding low-energy conformations.* © 1998 John Wiley & Sons, Inc. Biopoly 46: 155–167, 1998

Keywords: *α-MSH; [D-Phe[7]]α-MSH; isomerism; cyclic analogues*

Correspondence to: V. J. Hruby, Department of Chemistry, University of Arizona, Tucson, AZ 85721
Contract grant sponsor: U.S. Public Health Service
Contract grant number: DK17420
Biopolymers, Vol. 46, 155–167 (1998)

CCC 0006-3525/98/030155-13

INTRODUCTION

The tridecapeptide α-melanotropin (α-MSH, α-melanocyte stimulating hormone), Ac-Ser[1]-Tyr[2]-Ser[3]-Met[4]-Glu[5]-His[6]-Phe[7]-Arg[8]-Trp[9]-Gly[10]-Lys[11]-Pro[12]-Val[13]-NH_2, is a stimulator of melanogenesis in mouse and human melanocytes, mouse B16 and Cloudman S91 melanoma cells, as well as a stimulator of tyrosinase induction in some human melanoma cell lines (e.g., Ref. 1). The structure–function and conformation–function relationships for α-MSH for interaction with pigment cell receptors has been intensely studied in the last two decades by synthesis and biological studies of various α-MSH analogues.[1–3] It has been shown that the minimal sequence possessing α-MSH-like activity is the central tetrapeptide His[6]-Phe[7]-Arg[8]-Trp[9] (Ref. 4). This ''core'' sequence was suggested to be the ''message'' fragment for α-MSH, the rest of the molecule being regarded as the ''address'' sequence[5] (some authors have suggested that the C-terminal Lys[11]-Pro[12]-Val[13]-NH_2 fragment also contributes to the α-MSH message).[6,7] Linear superagonists of α-MSH with prolonged action were obtained by substitution of the Phe[7] residue for its D-enantiomer and replacing Met[4] with Nle[4] (Ref. 8). This finding became the basis of the suggestion that the central His[6]-Phe[7]-Arg[8]-Trp[9] message sequence of α-MSH adopts a β-turn or β-turn-like structure when bound to α-MSH specific receptors.[9] The peptide chain reversal of this kind could bring the side chains in positions 4 and 10 in close proximity, which was the reason for the synthesis of cyclic [half-Cys[4], half-Cys[10]]-α-MSH.[9,10] This analogue and its fragments generally were found to be more active than their linear counterparts in both frog and lizard skin bioassays.[9,10] Furthermore, they generally were less potent compared to the same cyclic fragments with the additional substitution of the Phe[7] for D-Phe[7] (Ref. 11).

A comparison of the nmr data and biological activity results for α-MSH analogues with subsequent substitutions of each amino acid residue in the His[6]-Phe[7]-Arg[8]-Trp[9] fragment yielded a model that suggested the predominant β conformations for the residues in this fragment (i.e., those with $\phi = -139°$, $\psi = 135°$ for L-, and with $\phi = 139°$, $\psi = -135°$ for D-amino acid residues).[12] At the same time, energy calculations for α-MSH and its [half-Cys[4], half-Cys[10]] cyclic analogue led to the conclusion that the biologically active conformation of α-MSH might be stabilized with either Glu[5]···Arg[8] or Glu[5]···Lys[11] salt bridges between oppositely charged ionic side chains of the molecule.[13,14] To test both hypotheses, the cyclic lactam analogues Ac-Nle[4]-cyclo[D-Orn[5], Glu[8]]α-MSH(4–11)NH_2 and Ac-Nle[4]-cyclo[D-Orn[5], D-Phe[7], Glu[8]]α-MSH(4–11)NH_2, were synthesized, the former retaining the potency of the corresponding linear fragment of α-MSH in frog skin bioassays and the latter possessing more than 100-fold less potency.[15] More recently, quenched molecular dynamics simulations performed on α-MSH and its [Nle[4], D-Phe[7]] analogue suggested the possibility of the close spatial location of residues in positions 5 and 10.[16] Accordingly, another cyclic lactam analogue, Ac-Nle[4]-cyclo[Asp[5], D-Phe[7], Lys[10]]α-MSH(4–10)NH_2, was synthesized and was found to be exceptionally potent in melanoma tyrosinase assays, demonstrating pronounced selectivity and prolongation of action.[16,17] On the contrary, the N-terminal to C-terminal cyclic hexapeptides cyclo(Gly-His-Phe-Arg-Trp-Gly) and cyclo(Gly-His-D-Phe-Arg-Trp-Gly) were significantly less potent than their linear precursors in frog skin assays.[18]

This data on cyclic analogues of α-MSH resulted in a variety of models for the spatial structure of α-MSH and its central fragment analogues. Some of these models have been examined by energy calculations,[14,16] but a systematic conformational search for α-MSH was performed just once,[13] using rather out-of-date force field parameters.[19] The main goal of this paper is to examine and refine a model for the ''biologically active'' backbone conformer of the message sequence of α-MSH employing energy calculations, followed by synthesis of conformationally constrained analogues of α-MSH, and studies of their biological activity to examine the validity of these models. First, we have performed systematic energy calculations for α-MSH and its [D-Phe[7]] analogue to find their low energy conformations. Then we have used the knowledge obtained from these low-energy conformations to design and to synthesize new cyclic analogues of α-MSH. Finally, the biological activities of these analogues were examined, and, independently, sets of low energy conformers for the analogues were found by energy calculations. Analysis of the results of biological studies in light of energy calculations for cyclic analogues allowed us to further refine the model for the biologically active backbone conformers of the message sequence of α-MSH, as well as to reach some conclusions concerning the molecular mechanisms of interaction between α-MSH analogues and its pigment cell receptors.

GENERAL METHODS

The protected amino acid derivatives and the *p*-methylbenzhydrylamine peptide resin were obtained from Bachem (Torrance, CA). Thin-layer chromatography

Table I Analytical Properties of New Cyclic Analogues of α-MSH

Analogue[d]	$[\alpha]_{589}^{23}$ in 10% AcOH (deg)	TLC R_f Values[a] A	B	C	HPLC[b] K'	FAB-MS (M + H) Found	Calculated	Amino Acid Analysis[c]
Ia	−43.8 (c, 0.041)	0.78	0.07	0.69	8.41 (a) 3.19 (d)	982.5	983.1	Asp(0.92), His(0.94), Phe(1.0), Arg(1.1), Ala(1.08), Lys(0.93)
Ib	−56.2 (c, 0.035)	0.75	0.06	0.67	3.88 (a)	1096.5	1096.27	Nle(1.0), Asp(0.91), His(0.96), Phe(1.03), Arg(1.05), Ala(1.1), Lys(0.93)
IIa	−23.5 (c, 0.033)	0.77	0.07	0.7	6.56 (e) 6.21 (d)	982.7	983.1	Asp(0.90), His(0.96), Phe(1.0), Arg(1.1), Ala(1.04), Lys(0.92)
IIIa	−40 (c, 0.029)	0.79	0.08	0.71	5.97 (e) 3.34 (d)	982.5	983.1	Asp(0.90), His(0.98), Phe(1.0), Arg(0.97), Ala(0.95), Lys(0.94)
IIIb	−45.2 (c, 0.044)	0.79	0.07	0.70	3.34 (a) 3.95 (b)	1096.5	1096.27	Nle(1.1), Asp(0.95), His(0.92), Phe(1.0), Arg(1.02), Ala(1.01), Lys(0.91)
IVa	−21.8 (c, 0.032)	0.74	0.08	0.67	8.62 (f) 1.96 (a)	982.4	983.1	Asp(0.92), His(0.97), Phe(1.0), Arg(0.94), Ala(1.1), Lys(0.95)
IVb	−46.1 (c, 0.048)	0.73	0.06	0.65	6.39 (a)	1095.6	1096.27	Nle(1.0), Asp(0.90), His(0.91), Phe(1.1), Arg(1.05), Ala(1.08), Lys(0.91)
Va	−30.7 (c, 0.045)	0.78	0.09	0.70	5.46 (c) 4.1 (d)	997	997.1	Asp(0.89), His(0.97), Phe(1.0), Arg(1.1), Lys(0.92)
Vb	−31.2 (c, 0.041)	0.76	0.08	0.68	5.89 (a)	1110	1110.3	Nle(1.0), Asp(0.90), His(0.97), Phe(1.06), Arg(0.98), Lys(0.90)
Vc	−38.5 (c, 0.023)	0.78	0.08	0.71	9.33 (f)	996.5	997.1	Asp(0.88), His(0.99), Phe(1.0), Arg(1), Lys(0.90)
Vd	−42.3 (c, 0.03)	0.77	0.07	0.69	3.87 (b)	1110	1110.3	Nle(0.96), Asp(0.93), His(0.90), Phe(1.0), Arg(0.94), Lys(0.95)
VIa	−33.4 (c, 0.047)	0.82	0.09	0.73	0.74 (a) 8.26 (f)	982.5	983.1	Asp(0.96), His(0.93), Phe(1.0), Arg(0.97), Lys(0.93)
VIb	−46.2 (c, 0.037)	0.80	0.08	0.70	2.37 (b) 9.5 (e)	1096	1096.27	Nle(1.1), Asp(0.94), His(0.96), Phe(1.0), Arg(1.0), Lys(0.90)
VIc	−28.8 (c, 0.031)	0.84	0.07	0.73	0.91 (a) 4.31 (c)	983.5	983.1	Asp(0.88), His(1.03), Phe(1.0), Arg(1.0), Lys (0.93)
VId	−31.6 (c, 0.035)	0.81	0.05	0.72	3.17 (a) 2.89 (b)	1097	1096.27	Nle(1.0), Asp(0.90), His(0.96), Phe(1.1), Arg(0.97), Lys(0.95)
VIIa	−51.1 (c, 0.029)	0.79	0.07	0.68	581 (e) 2.16 (c)	983	983.1	Asp(0.90), His(0.92), Phe(1.0), Arg(0.99), Ala(1.0), Lys(0.90)
VIIb	−4.53 (c, 0.024)	0.77	0.06	0.68	1.24 (b)	1096.5	1096.27	Nle(0.97), Asp(0.94), His(0.97), Phe(1.0), Arg(0.94), Ala(1.1), Lys(0.89)

[a] Solvent systems: (A) 1-butanol/AcOH/pyridine/H_2O (5:1:5:4), (B) EtOAc/pyridine/AcOH/H_2O (5:5:1:3), (C) 1-butanol/AcOH/H_2O (4:1:1, upper phase).

[b] Analytical HPLC was performed on a C-18 column (VYDAC Cat. No. 218TP104) using a gradient of CH_3CN in 0.1% aq. TFA in 30 min at 1.5 mL/min. The following gradients were used: (a) 20–30%, (b) 20–40%, (c) 15–25%, (d) 15–30%, (e) 10–30%, and (f) 10–25%.

[c] Relative ratios in parentheses. Trp, Sar, and Aib not determined.

[d] For structures see Table 4.

(TLC) was performed on Merck silica gel 60 F_{254} plates in various solvent systems described at the end of Table I. Peptide spots on the developed plates were detected by uv and iodine vapor. Purification of the peptides was accomplished by semipreparative high performance liquid chromatography (HPLC) using a C-18 reversed-phase VYDAC column (218TP1010, 250 × 10 mm). The purity of the finished peptides was confirmed by reversed-phase analytical HPLC at λ280 and λ220 nm. Various gradient systems of CH_3CN in 0.1% aq. trifluoroacetic acid (TFA) were used and are described at the end of Table I. The purity of all the peptides ranged 90–96%. The structures of the peptides were confirmed by amino acid analysis and fast atom bombardment mass spectrometry (FAB-MS). Amino acid analysis was performed on an Applied Biosystems Model 420A amino acid analyzer with automatic peptide hydrolysis capability (vapor phase hydrolysis using 6N HCl at 160°C for 100 min). No correction was made for destruction of amino acids during hydrolysis. Optical rotations were measured on a Fisher Autopol III instrument at λ589 nm in 10% AcOH.

Table II Buildup Procedure for α-MSH and [D-Phe^7]α-MSH

		Number of Conformers	
Step	Fragment Considered	Considered	Selected
1	His-Phe-Arg-Trp-Gly	5000	533
	His-D-Phe-Arg-Trp-Gly	5000	677
2	Glu-His-Phe-Arg-Trp-Gly-Lys	13,325	28
	Glu-His-D-Phe-Arg-Trp-Gly-Lys	16,925	23
3	Met-Glu-His-Phe-Arg-Trp-Gly-Lys-Pro-Val-NH_2	1260	260
	Met-Glu-His-D-Phe-Arg-Trp-Gly-Lys-Pro-Val-NH_2	1035	200
4	Ser-Met-Glu-His-Phe-Arg-Trp-Gly-Lys-Pro-Val-NH_2	1300	154
	Ser-Met-Glu-His-D-Phe-Arg-Trp-Gly-Lys-Pro-Val-NH_2	1000	235
5	Ac-Ser-Tyr-Ser-Met-Glu-His-Phe-Arg-Trp-Gly-Lys-Pro-Val-NH_2	2310	157
	Ac-Ser-Tyr-Ser-Met-Glu-His-D-Phe-Arg-Trp-Gly-Lys-Pro-Val-NH_2	3525	99

EXPERIMENTAL METHODS

Energy Calculations

The methods and parameters used for energy calculations for α-MSH and its analogues were the same as we have used for opioid peptides.[20] Rigid valence geometries for the Sar and Aib residues were calculated employing the SYBYL program and the values of partial atomic charges for these residues were calculated by the Del Re technique (SYBYL implementation).[21] All peptide bonds were assumed to be in the rigid planar *trans* conformations, except that preceding the Sar residues, where the ω angle was allowed to rotate and to choose from both *trans* and *cis* possibilities. The patterns of energy calculations for α-MSH and [D-Phe^7]α-MSH were based on a buildup procedure for ''growing'' of the peptide chain. Three of the amino acid side chain functional groups were regarded as ionized, namely the γ-carboxyl of the Glu^5, the guanidino group of the Arg^8, and the ε-amino group of the Lys^{11}. The buildup procedure was started from the central pentapeptide 6–10 to the fragment 5–11 (which contains all ionized functional groups in question) and then subsequently to the fragments 4–13 and 2–13, and to the entire molecule (Table II). The starting points for energy minimization in the first step were the backbone conformations corresponding to the dihedral angle values of $\phi = -140°$, $\psi = 140°$; $\phi = -75°$, $\psi = 140°$; $\phi = -75°$, $\psi = 80°$; $\phi = -60°$, $\psi = -60°$; $\phi = 60°$, $\psi = 60°$ for all L-amino acid residues; and to the same values with reversed signs for the D-amino acid residues. For the Gly residue the starting points were obtained by combinations of those for both L- and D-amino acid residues, and for Pro residue they were $\psi = 140°$, 80°, and $-60°$ ($\phi_{Pro} = -75°$). The same starting points were used for new residues attached to the conformers selected at the previous steps. The backbone conformers selected for further consideration at the each step were those satisfying the criteria of $\Delta E = E - E_{min} \leq 10$ kcal/mol, except for the last three steps, where the ΔE values were 12 kcal/mol. At each step the spatial arrangement of the side chains was optimized before energy minimization by a special algorithm (see Ref. 20 for details).

Energy calculations for cyclic analogues Ac-cyclo[L/D-Asp^5, L/D-Phe^7, X^{10}, Lys^{11}]α-MSH(5–11)NH_2 (X = Ala, D-Ala, Sar, Aib) were performed according to a somewhat different buildup procedure (Table III). First, the conformers of the peptide backbone for the 5–11 fragment possessing a distance between C^{β}_5 and C^{β}_{11} atoms less than 7 and more than 4 Å were selected using all possible combinations of starting points described above. Then the low-energy conformations of the cyclic peptide backbone, where all nonglycine residues except the L/D-Asp^5 and Lys^{11} were replaced by alanines, were obtained. Starting from this step, all ω angles inside a cycle were allowed to rotate during energy minimization. In most cases, the final step for the cyclic molecules was performed as two simultaneous independent substeps (see Table III). One option was to replace the β-methyl groups of all alanines (but not for the glycine) by the corresponding side chains, to perform energy calculations, and then to replace the Gly^{10} residue by the X^{10} residues (X = Ala, D-Ala, Sar, Aib) for the conformers selected by the $\Delta E = 10$ kcal/mol criteria. Another way was first to replace the Gly^{10} residue by the X^{10} residues, preserving alanines, and then to replace the alanines. Finally, both obtained sets of conformations for each of the cyclic molecules were merged and low-energy conformers were selected (Table III). In the case of Ac-cyclo[Asp^5, D-Phe^7, Aib^{10}, Lys^{11}]α-MSH(5–11)NH_2, additional energy minimizations starting from the final sets of low-energy conformers for Ac-cyclo[Asp^5, Phe^7, Ala^{10}, Lys^{11}]α-MSH(5–11)NH_2 and Ac-cyclo[Asp^5, Phe^7, D-Ala^{10}, Lys^{11}]α-MSH(5–11)NH_2 were performed also. The final set of conformers was selected by merging of all calculated conformers for this analogue which satisfy the energy criterium $\Delta E < 12$ kcal/mol.

Geometrical Comparison

The geometrical similarity between a pair of conformers was checked by the assessment of the best fit of the spatial

Table III Buildup Procedure for Cyclic Analogues of α-MSH and [D-Phe^7]α-MSH

Analogue	Step	Sequence Considered	No. of Conformers Considered	No. of Conformers Selected
Ia	1	Ac-Asp-Ala-**Ala**-Ala-Ala-**Gly**-Lys-NH_2	2572[a]	242
	2	Ac-c[Asp-His-**Phe**-Arg-Trp-**Gly**-Lys]-NH_2	242	31
	2′	Ac-c[Asp-Ala-**Ala**-Ala-Ala-**Ala**-Lys]-NH_2	242	155
	3	Ac-c[Asp-His-**Phe**-Arg-Trp-**Ala**-Lys]-NH_2	31	11
	3′	Ac-c[Asp-His-**Phe**-Arg-Trp-**Ala**-Lys]-NH_2	155	32
	4	Ac-c[Asp-His-**Phe**-Arg-Trp-**Ala**-Lys]-NH_2	11 + 32	35
IIa	1	Ac-Asp-Ala-**D-Ala**-Ala-Ala-**Gly**-Lys-NH_2	5628[a]	260
	2	Ac-c[Asp-Ala-**D-Ala**-Ala-Ala-**D-Ala**-Lys]-NH_2	260	128
	3	Ac-c[Asp-His-**D-Phe**-Arg-Trp-**D-Ala**-Lys]-NH_2	128	56
IIIa	2	Ac-c[Asp-His-**D-Phe**-Arg-Trp-**Gly**-Lys]-NH_2	260	26
	2′	Ac-c[Asp-Ala-**D-Ala**-Ala-Ala-**Ala**-Lys]-NH_2	260	191
	3	Ac-c[Asp-His-**D-Phe**-Arg-Trp-**Ala**-Lys]-NH_2	26	10
	3′	Ac-c[Asp-His-**D-Phe**-Arg-Trp-**Ala**-Lys]-NH_2	191	16
	4	Ac-c[Asp-His-**D-Phe**-Arg-Trp-**Ala**-Lys]-NH_2	10 + 16	21
IVa	1	Ac-Asp-Ala-**D-Ala**-Ala-**D-Ala**-**Ala**-Lys-NH_2	5847[a]	616
	2	Ac-c[Asp-His-**D-Phe**-Arg-**D-Trp**-**Ala**-Lys]-NH_2	616	88
Va	3	Ac-c[Asp-His-**D-Phe**-Arg-Trp-**Aib**-Lys]-NH_2	26	15
	2′	Ac-c[Asp-Ala-**D-Ala**-Ala-Ala-**Aib**-Lys]-NH_2	260	111
	3′	Ac-c[Asp-His-**D-Phe**-Arg-Trp-**Aib**-Lys]-NH_2	111	42
	4	Ac-c[Asp-His-**D-Phe**-Arg-Trp-**Aib**-Lys]-NH_2	15 + 42	48
	4′	Ac-c[Asp-His-**D-Phe**-Arg-Trp-**Aib**-Lys]-NH_2	21 + 56	46
VIa[b]	3	Ac-c[Asp-His-**D-Phe**-Arg-Trp-**Sar**-Lys]-NH_2	26	7
	2′	Ac-c[Asp-Ala-**D-Ala**-Ala-Ala-**Sar**-Lys]-NH_2	260	118
	3′	Ac-c[Asp-His-**D-Phe**-Arg-Trp-**Sar**-Lys]-NH_2	118	6
	4	Ac-c[Asp-His-**D-Phe**-Arg-Trp-**Sar**-Lys]-NH_2	7 + 6	8
VIa[c]	1	**Ac-Asp-Ala-D-Ala**-Ala-Ala-**Sar**-Lys-NH_2	6819[a]	39
	2	Ac-c[Asp-His-**D-Phe**-Arg-Trp-**Sar**-Lys]-NH_2	39	14
VIa[d]	Final	**Ac-c[Asp-His-D-Phe**-Arg-Trp-**Sar**-Lys]-NH_2	8 + 14	7
VIIa	1	Ac-**D-Asp**-Ala-**D-Ala**-Ala-Ala-**Ala**-Lys-NH_2	5502[a]	45
	2	Ac-c[**D-Asp**-His-**D-Phe**-Arg-Trp-**Ala**-Lys]-NH_2	45	9

[a] The number of conformers with $C^{\beta}_{5} - C^{\beta}_{11}$ distance less than 7.0 Å and greater than 4.0 Å.
[b] Sar in *trans* conformation.
[c] Sar in *cis* conformation.
[d] Sar both in *trans* and *cis* conformations.

arrangement for selected atomic centers (see also Ref. 20). In all cases the conformers were regarded as similar when the rms value for these atomic centers was less than 1.0 Å.

Peptide Synthesis

All peptides were synthesized by solid phase methods of peptide synthesis[22] on a Vega 250 peptide synthesizer. The procedures employed were very similar to that described for the synthesis of cyclic lactam bridge-containing melanotropin analogues on a solid support.[17] In brief, individual amino acids as their N^{α}-*t*-butyloxycarbonyl (Boc) protected derivatives were successively coupled to *p*-methylbenzhydrylamine (pMBHA) resin (substitution 0.3–0.4 mmol/g resin) using diisopropylcarbodiimide-*N*-hydroxybenzotriazole (DIC-HOBt) as coupling reagents. The side-chain protecting groups on the Lys (or D-Lys) and Asp (or D-Asp) residues were fluorenylmethoxycarbonyl (Fmoc) and fluorenylmethyl ester (OFm), respectively, which are stable under the acidic conditions (50% TFA in dichloromethane) usually employed for removal of the N^{α}-Boc group. After complete synthesis of the linear protected peptide on the resin, both Fmoc and OFm groups were removed by treatment of the peptide resin for 20 min with 20% piperidine in *N*-methylpyrrolidinone. Then the liberated carboxyl and amino functional groups were coupled using BOP reagent[23] to construct the cyclic lactam peptide on the resin. In each case the peptide was released from the resin by treating with 10 mL/gm resin of a mixture of hydrogen fluoride (HF)-anisole (9:1). All the crude peptides were subjected to purification by preparative HPLC and purity

Table IV Biological Potencies of Cyclic Analogues of α-MSH in Frog Skin Bioassays

Analogue	Sequence	Potency[a]
α-MSH	Ac-Ser-Tyr-Ser-Met-Glu-His-Phe-Arg-Trp-Gly-Lys-Pro-Val-NH_2	1.00
Ia	Ac-cyclo(Asp-His-**Phe**-Arg-Trp-**Ala**-Lys)-NH_2	0.002
Ib	Ac-Nle-cyclo(Asp-His-**Phe**-Arg-Trp-**Ala**-Lys)-NH_2	0.016
IIa	Ac-cyclo(Asp-His-D-Phe-Arg-Trp-**D-Ala**-Lys)-NH_2	0.0014
IIIa	Ac-cyclo(Asp-His-D-Phe-Arg-Trp-**Ala**-Lys)-NH_2	0.37
IIIb	Ac-Nle-cyclo(Asp-His-D-Phe-Arg-Trp-**Ala**-Lys)-NH_2	0.917
IVa	Ac-cyclo(Asp-His-D-Phe-Arg-**D-Trp-Ala**-Lys)-NH_2	0.011
IVb	Ac-Nle-cyclo(Asp-His-D-Phe-Arg-**D-Trp-Ala**-Lys)-NH_2	0.48
Va	Ac-cyclo(Asp-His-D-Phe-Arg-Trp-**Aib**-Lys)-NH_2	0.25
Vb	Ac-Nle-cyclo(Asp-His-D-Phe-Arg-Trp-**Aib**-Lys)-NH_2	1.00
Vc	Ac-cyclo(Asp-His-D-Phe-Arg-Trp-**Aib-D-Lys**)-NH_2	0.008
Vd	Ac-Nle-cyclo(Asp-His-D-Phe-Arg-Trp-**Aib-D-Lys**)-NH_2	0.01
VIa	Ac-cyclo(Asp-His-D-Phe-Arg-Trp-**Sar**-Lys)-NH_2	0.01
VIb	Ac-Nle-cyclo(Asp-His-D-Phe-Arg-Trp-**Sar**-Lys)-NH_2	0.005
VIc	Ac-cyclo(Asp-His-D-Phe-Arg-Trp-**Sar-D-Lys**)-NH_2	0.001
VId	Ac-Nle-cyclo(Asp-His-D-Phe-Arg-Trp-**Sar-D-Lys**)-NH_2	0.023
VIIa	Ac-cyclo(**D-Asp**-His-D-Phe-Arg-Trp-**Ala**-Lys)-NH_2	0.02
VIIb	Ac-Nle-cyclo(**D-Asp**-His-D-Phe-Arg-Trp-**Ala**-Lys)-NH_2	0.001

[a] Relative to α-MSH = 1.00.

was confirmed by reversed-phase analytical HPLC. The peptides were characterized by fast atom bombardment mass spectrometry, HPLC, TLC, and amino acid analysis, and the analytical data for the purified peptides are given in Table I.

Biological Screening

Bioassays were performed on frog (*Rana pipiens*) skins according to published methods.[24–26] In these assays the darkening of skin due to dispersion of melanin granules within the melanocytes in response to melanotropin analogues is measured by photoreflectance methods. The potency of each analogue was determined from the dose–response curves comparing the skin darkening with that caused by the native hormones, α-MSH. The comparative biological activities are given in Table IV.

RESULTS

Energy Calculations for α-MSH and [D-Phe^7]α-MSH

Energy calculations for α-MSH and [D-Phe^7]α-MSH molecules were performed according to the buildup procedure in Table II. At the very last step of this procedure, the low-energy structures obtained earlier for the entire molecules of α-MSH and [D-Phe^7]α-MSH (71 and 74 structures, respectively) used in the preliminary publication[27] were reminimized and combined with the structures obtained following the pattern of Table II. This yielded 157 different backbone structures for α-MSH, satisfying the criterion of $\Delta E < 12$ kcal/mol, and 99 different low-energy backbone structures for [D-Phe^7]α-MSH. (The term ''different'' means that each of the structures differs from all others by more than 60° in the value of at least one of the backbone dihedral angles).

It is convenient to divide the obtained low-energy structures of α-MSH and [D-Phe^7]α-MSH into several structure types according to the possible geometrical shapes of the message sequences His-L/D-Phe-Arg-Trp. Indeed, many of low energy structures of α-MSH and [D-Phe^7]α-MSH showed geometrical similarity in spatial arrangements for C^α and C^β atoms in His-L/D-Phe-Arg-Trp fragments with rms values <1 Å, when compared to each other according to Experimental Methods section. The comparison revealed 5 different structural types for α-MSH and 8 types for [D-Phe^7]α-MSH. The most populated are structure types, *1*, *2*, and *3* for α-MSH (154 structures out of 157) and *1–6* for [D-Phe^7]α-MSH (96 structures out of 99); only these structure types will be discussed below. The backbone dihedral angles for fragments 6–9, corresponding to the lowest energy structure for each structure type are listed in Table V along with number of conformers belonging to each structure type. Since both α-MSH and [D-Phe^7]α-MSH are highly active

Table V Types of Conformers for Message Sequence of α-MSH and [D-Phe^7]α-MSH, Differing in Spatial Arrangements of Side-Chain Functional Groups

Peptide	Type	His		L/D-Phe		Arg		Trp		No. of Conformers
		ϕ	ψ	ϕ	ψ	ϕ	ψ	ϕ	ψ	
α-MSH	1	−61	−38	−78	−27	−71	93	−91	−27	82
	2	−70	−33	−91	−23	−82	−33	58	70	64
	3	−70	−31	−82	−27	−69	135	66	28	8
[D-Phe^7]-α-MSH	1	−70	120	84	17	−102	142	−70	134	18
	2	−142	135	75	18	−139	123	55	46	25
	3	−66	100	122	−21	−99	−60	55	69	29
	4	47	53	114	−57	−166	139	−61	−51	6
	5	−68	151	51	−122	−161	86	−98	−22	8
	6	−62	112	78	17	−154	38	−67	−56	13

molecules, they could be expected to possess similar geometrical shapes of their ''message'' sequences, which participate in receptor binding. Geometrical comparison of low energy structures for α-MSH with those for [D-Phe^7]α-MSH, performed with the same atomic centers and in the same way as described above, pointed out two possible variants of similarity in question. First, the conformers of type *1*, and partly, of type *2* for α-MSH are similar to the conformers of type *3* for [D-Phe^7]α-MSH, and, second, the conformers of type *3* for α-MSH are similar to the conformers of type *2* for [D-Phe^7] α-MSH. Both cases of similarity are depicted in Figures 1a and b, which show the corresponding structure types overlapped.

The two conformer types mentioned above can be regarded as possible alternative models for the conformation of the His-L/D-Phe-Arg-Trp message sequence, which is presumably involved in receptor binding, i.e., the models for the biologically active conformation. To achieve the best results in design of the analogues with the additional stabilization of these conformations, one can consider the following: (a) the side chains in the message sequence should not be modified [1,3]; (b) analogues with D-Phe^7 are expected to be more potent than their counterparts with L-Phe^7, which has been the case for numerous other α-MSH analogues (see, e.g., Ref. 8); and (c) the side chains of amino acid residues in positions 5 and 11 could be placed in near proximity and covalently linked together to create conformationally constrained cyclic analogues with the cyclization between the position 5 and 11 (see Figure 1). It seems also reasonable to substitute the conformationally flexible Gly^{10} residue (''the conformational hinge'' [27]) by more constrained residues to further stabilize different conformations of the message sequence. In this view the ''minimal'' substitutions would be the different kinds of replacements of hydrogen atoms in position 10 for methyl groups, i.e., the substitutions of Gly^{10} for the L/D-Ala, Aib, or Sar residues.

The above considerations were the basis for design of a series of cyclic analogues of [D-Phe^7]α-MSH with the general sequence of X-cyclo(Asp-His-D-Phe-Arg-Trp-Y-Lys)-NH_2, where X = Ac, Ac-Nle and Y = Ala, D-Ala, Aib or Sar. We have decided also to synthesize several additional cyclic analogues with enantiomers of the Asp, Phe, Trp, and Lys residues (for the entire list of synthesized analogues see Table IV). Our main goal was to provide additional experimental data for refining the model of the biologically active conformation of α-MSH message sequence, and in this sense, to make a distinction between different conformer types for α-MSH and [D-Phe^7]α-MSH. It should be noted that this goal is unlikely to be achieved by nmr studies of these cyclic peptides since they undoubtedly are flexible enough to display some conformational averaging in solution.

Synthesis of Cyclic Analogues

The cyclization of the peptide analogues on the resin proceeded very well. All the peptides were obtained in good yields (12–38%) after purification to homogeneity by preparative HPLC. The peptides exhibited correct molecular ion peaks in FAB-MS and gave satisfactory amino acid analyses (Table I).

Biological Testing of Cyclic Analogues

The relative potencies of the peptides to darken frog skins are given in Table IV. It was interesting to

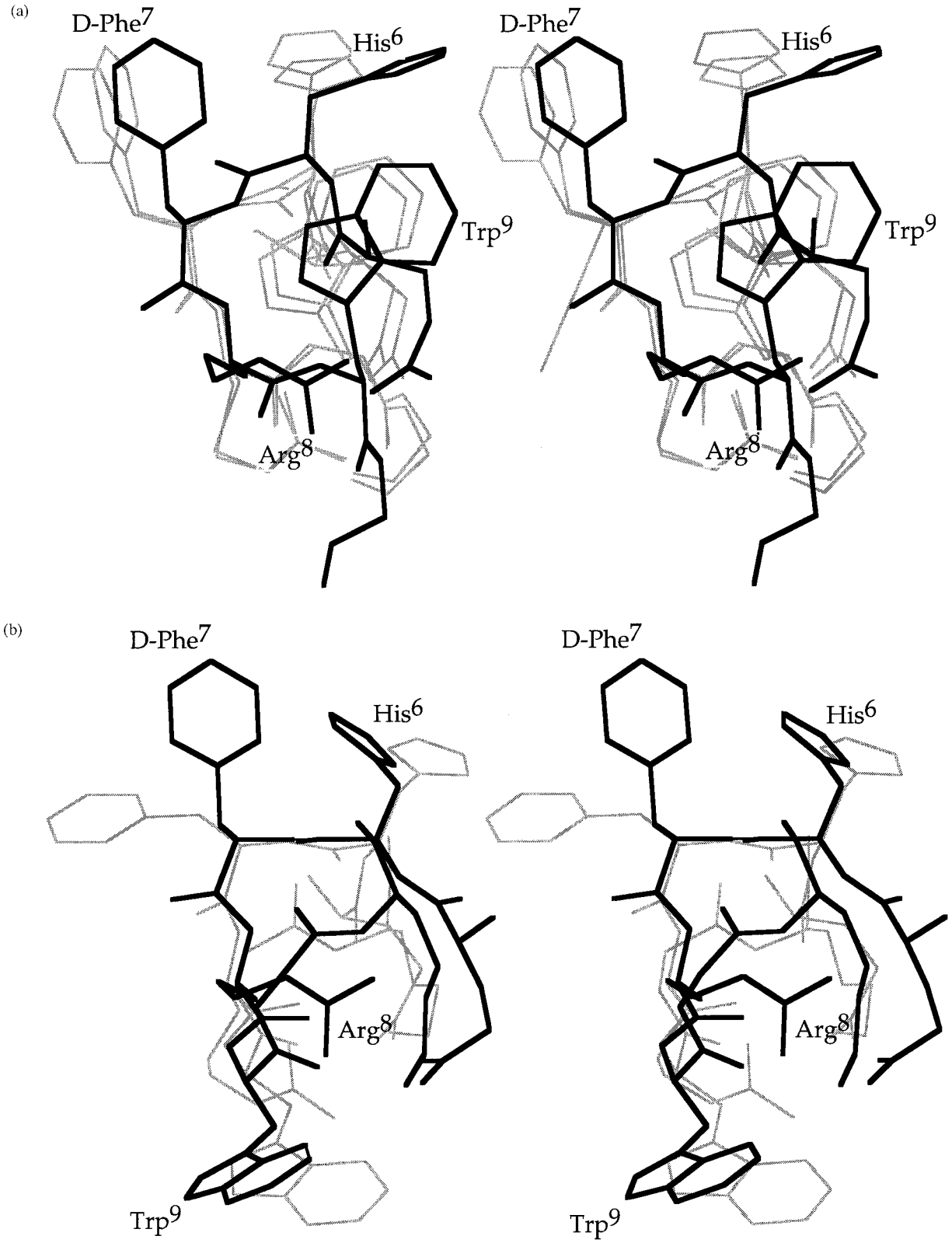

FIGURE 1 Stereoview of overlapping of the 5–11 fragments for [D-Phe^7]α-MSH (thick black line) and α-MSH (thin shadow lines) for structure types *3*, and *1* and *2* (a); and *2* and *3* (b), respectively. All hydrogens are omitted for clarity.

Table VI Low-Energy Conformers of α-MSH (A) and [D-Phe^7]α-MSH (B) and of Cyclic Analogues, Similar in Spatial Arrangements of Side-Chain Functional Groups for the Message Sequence

		Asp	His		L/D-Phe		Arg		L/D-Trp		X[b]		Lys	
Peptide	No.[a]	ψ	φ	ψ	φ	ψ	φ	ψ	φ	ψ	φ	ψ	φ	ΔE (kcal/mol)
A	1	−44	−61	−38	−78	−27	−71	93	−91	−27	−78	79	−152	0.0
	16	−35	−67	−41	−75	−27	−80	−29	59	67	68	−122	55	6.1
B	14	−19	−66	110	114	−9	−116	−62	57	66	71	41	−140	5.8
Ia	11	−40	−66	−42	−66	−47	−85	78	−65	−38	−76	80	−79	5.5
IIa	9	−30	−60	151	94	−60	−64	−47	−95	140	−55	−58	51	3.9
	18	−55	−70	−40	−50	−60	−85	135	−71	139	76	54	58	5.2
IIIa	1	−33	−58	130	101	−39	−74	−40	−112	146	−78	78	−80	0.0
	14	−38	−59	−46	−52	−48	−67	−52	−147	134	−68	137	−85	9.1
	20	−46	−65	−41	−47	−67	−85	77	−61	−36	−74	79	−74	9.8
IVa	19	140	−65	150	105	−71	−81	−46	121	−141	−89	128	−157	4.7
	21	−45	−67	−44	−47	−56	−87	72	−54	−44	−74	80	−76	4.8
	82	153	−112	150	86	−125	49	54	91	−85	−147	101	−156	8.8
Va	7	−34	−58	129	103	−38	−76	−39	−112	145	−73	72	−82	5.0
	31	−47	−67	−39	−47	−71	−87	71	−66	−31	−62	70	−71	10.5
VIa	2	−32	−58	135	99	−44	−71	−38	−112	145	−77	72	−84	0.1
	5	−34	−60	146	96	−52	−68	−44	−101	150	−61	−57	52	8.5
VIIa	3	−80	−74	159	85	−68	−58	−45	−111	158	−76	83	−127	6.8
	4	−165	−66	149	90	−60	−64	−41	−112	151	−80	87	−114	7.1

[a] The number of a low-energy conformer in order of increasing ΔE values.
[b] X = Ala, D-Ala, Aib, or Sar.

observe that the analogues displayed greatly varied potencies that ranged from 1000-fold less potent to equipotent to α-MSH. In general, inclusion of Nle^4 caused a significant increase in potency of the peptides. Notable exceptions, however, were **VIb** and **VIIb,** where addition of a Nle^4 residue caused 2-fold and 20-fold drops in potency. As anticipated all the D-Phe-containing peptides were significantly more active than L-Phe-containing analogues. Interestingly, the linear analogue Ac-Nle-Gly-His-D-Phe-Arg-Trp-Gly-Lys-NH_2 made earlier[29] showed a bioactivity that is about 0.2 that of α-MSH,[29] whereas the cyclic analogue Ac-Nle-cyclo(Asp-His-D-Phe-Arg-Trp-Ala-Lys)-NH_2 (analogue **IIIb,** differs by an Ala instead of Gly at position 10), possess bioactivity that is 0.92 that of α-MSH (Table IV). Therefore it is reasonable to assume that the bioactive conformation is somewhat stabilized in the cyclic analogue.

DISCUSSION

Energy Calculations for Cyclic Analogues and Geometrical Comparisons

Seven types of cyclic analogues were selected for energy calculations, namely the analogues **I(a)**–**VII(a)** (Table IV). The calculations were performed according to the buildup procedure described in Experimental Methods section and in Tables II and III. The final lists of low-energy backbone conformations include 35 structures for analogue **Ia,** 56 for **IIa,** 21 for **IIIa,** 88 for **IVa,** 46 for **Va,** 7 for **VIa,** and 9 for **VIIa.** As might have been expected, no low energy conformer of Ala^{10}-containing analogues **Ia, IIIa, IVa,** and **VIIa** occupied a sterically forbidden region of the Ramachandran map with positive φ and negative ψ values in position 10; the same is true for the D-Ala^{10}-containing analogue **IIa,** where signs of dihedral angles φ and ψ in the sterically forbidden region in position 10 are reversed. Also, as expected, the *N*-methylated Sar^{10} residue has limited the conformational possibilities for the preceding Trp^9 residue to the structures with the positive ψ values found only in analogue **VIa;** no low energy analogues with a *cis* conformation of the Sar^{10} residue were found. At the same time, substitution of the Aib^{10} residue in analogue **Va** confined the possible conformations in position 10 not only to either right or left α-helices, and, perhaps, to the fully extended conformation, as might be expected,[28] but also revealed the possibility of inverse γ-turn conformations ($\phi \cong -60°$, $\psi \cong 70°$).

All low-energy conformers of cyclic analogues

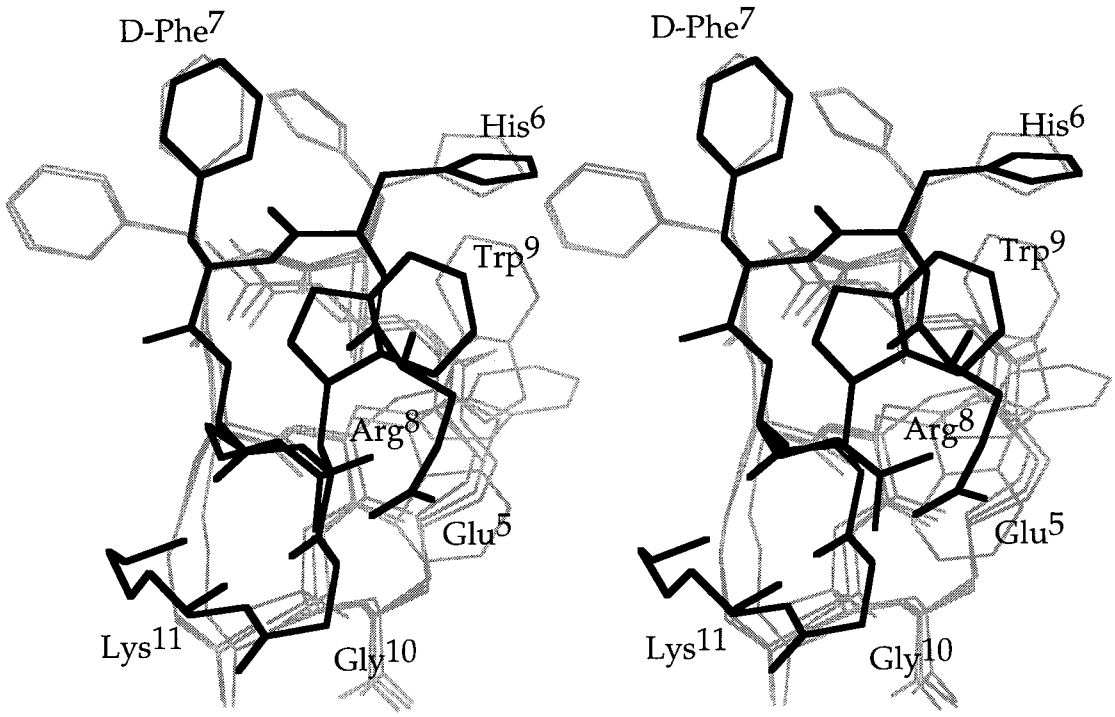

FIGURE 2 Stereoview of overlapping of conformer 20 for analogue **IIIa,** conformer 21 for analogue **IVa,** conformer 31 for analogue **Va** (thin shadow lines) and of backbone of fragment 5–11 for structure type *3* of [D-Phe^7]α-MSH (thick black line). All hydrogens are omitted for clarity.

were then compared to each other, as well as to the low-energy structures of α-MSH and [D-Phe^7]α-MSH. The comparison involved the spatial arrangements of their His-L/D-Phe-Arg-L/D-Trp fragments, using the same atomic centers and the same similarity criteria as were employed above for comparison of low-energy structures of α-MSH and [D-Phe^7]α-MSH. It was found that all cyclic analogues possess low energy conformers similar to each other and to the conformers of type *1* and *2* of α-MSH and of type *3* of [D-Phe^7]α-MSH as to the spatial arrangement of the central tetrapeptide message sequence. Table VI contains the dihedral angle values for backbones of those conformers together with their relative energies ΔE's, and with the corresponding ''template'' conformers of α-MSH and [D-Phe^7]α-MSH.

Most conformers of the cyclic peptides listed in Table VI are very close to each other as to the values of dihedral angles for their peptide backbones in the sequence from ψ_{His} to ϕ_{Trp} in the His-L/D-Phe-Arg-L/D-Trp fragment (the dihedral angles defining the mutual spatial arrangement of side chains in the fragment). Some discrepancies, like differences in ψ_{His} to $\phi_{D\text{-}Phe}$ values between conformers 1, 14, and 20 for analogue **IIIa,** could be overcome easily by rotation of the peptide bond plane between the His and D-Phe residues at ca. 180°, which would leave the mutual spatial positions of side chains for these two residues virtually unchanged. But the differences in dihedral angles outside of the His-L/D-Phe-Arg-L/D-Trp fragments can disrupt the overall spatial similarity between conformers. For instance, it is not possible to fully overlap conformers 1 and 14 with conformer 20 for analogue **IIIa** by any rotations of peptide bond planes due to the difference in the corresponding ψ_{Trp} values. Further, analyzing the conformers in Table VI, it can be deduced that there are two distinct groups of conformers with overall similarity. The first group is formed by conformer no. 11 for analogue **Ia,** no. 20 for **IIIa,** no. 21 for **IVa,** and no. 31 for **Va,** and the second one include conformers no. 9 for analogue **IIa** (with rotation of the peptide bond plane between the D-Ala and Lys residues), no. 1 for analogue **IIIa,** no. 7 for analogue **Va,** no. 2 for analogue **VIa,** and no. 3 for analogue **VIIa.**

Keeping in mind that analogues **IIIb, IVb,** and **Vb** can be considered as biologically potent (see the data in Table IV), whereas all other analogues

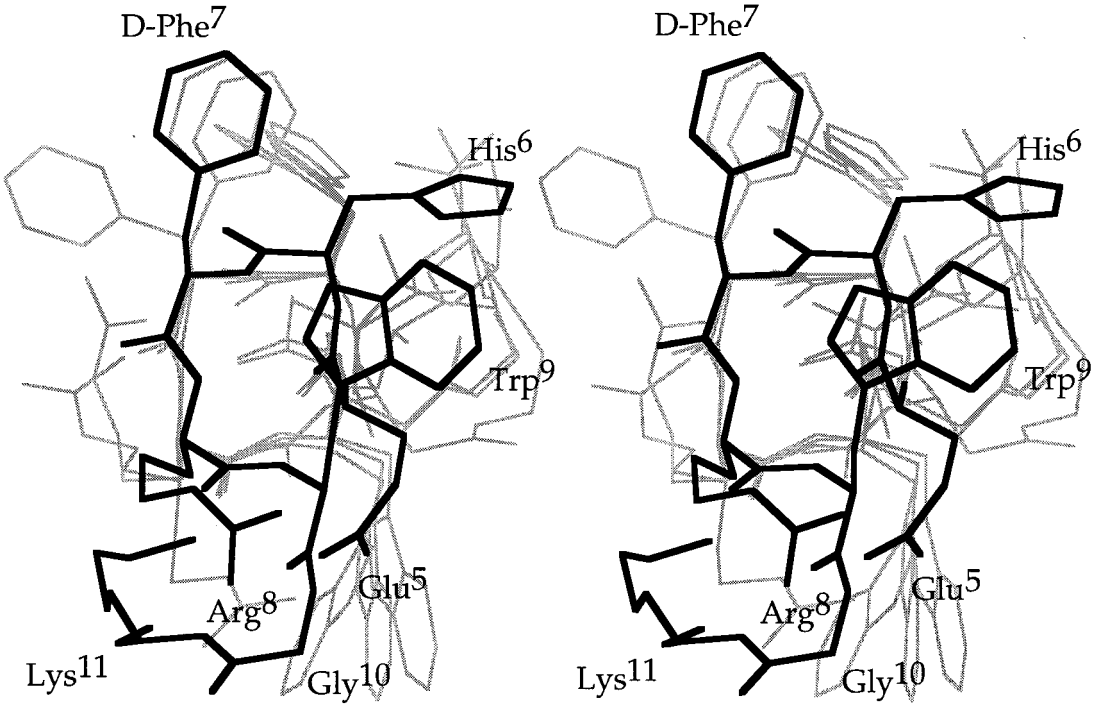

FIGURE 3 Stereoview of overlapping of conformer 9 for **IIa,** conformer 2 for **VIa,** conformer 3 for **VIIa** (thin shadow lines), and of the backbone of fragment 5–11 for structure type *3* of [D-Phe^7]α-MSH (thick black line). All hydrogens are omitted for clarity.

have reduced potency, it is noteworthy that the conformers of the first group are present in active analogues only, whereas conformers of the second group are present both in active and inactive cyclic analogues. The only exception (conformer 11 for analogue **Ia**) can be easily explained by the inherent difference in activity between α-MSH analogues containing L- or D-Phe^7 residues; the linear analogue Ac-[Nle^4, D-Phe^7]α-MSH(4–11)-NH_2 is 100 times more active than its L-Phe^7-containing counterpart.[18] This suggests that the first group of conformers can be used as a template for a model of the biologically active conformation for the α-MSH message sequence. These conformers are depicted overlapped in Figure 2 together with the corresponding backbone fragment of [D-Phe^7]α-MSH conformer of type *3*. The second group of conformers, which are characteristic for inactive analogues (conformer no. 9 for **IIa,** no. 2 for **VIa** and no. 3 for **VIIa**), are depicted in Figure 3 together with the same backbone conformer of [D-Phe^7]-α-MSH. In both Figures 2 and 3, the side chains of the His, D-Phe, Arg, and Trp residues do not occupy exactly the same spatial position for all depicted analogues, but they easily could be put more close together by limited rotations around side chain dihedral (χ_1 and/or χ_2) angles.

It is evident from Figure 2 (active analogues) that the aromatic side-chain moieties of the His^6, D-Phe^7, and Trp^9 residues can form a continuous ''surface,'' presumably interacting with a complementary receptor site. This feature is absent in the case of inactive analogues (Figure 3), since such a surface would be intersected by the lactam bridge and the backbone of the residue in position 10. This might be a factor which results in the loss of activity of **IIb, VIb,** and **VIIb** (assuming their cycle conformations would not be significantly changed after addition of the Nle^4 residues), despite the fact that some of low energy conformers for these analogues are geometrically similar to the same conformers of the ''message'' sequence for α-MSH and [D-Phe^7]α-MSH. The ability of the ''message'' sequence to form a continuous hydrophobic surface interacting with the receptor was mentioned earlier as a necessary feature of the α-MSH ''biologically active'' conformation.[27]

In summary, our findings allow us to refine a model for the biologically active conformation for the α-MSH message sequence. We are suggesting for this model that conformers no. 20 for **IIIa,** no. 21 for **IVa,** and no. 31 for **Va,** as well as the corresponding conformers of α-MSH and [D-Phe^7]α-MSH, listed in Table VI, are the most likely. It

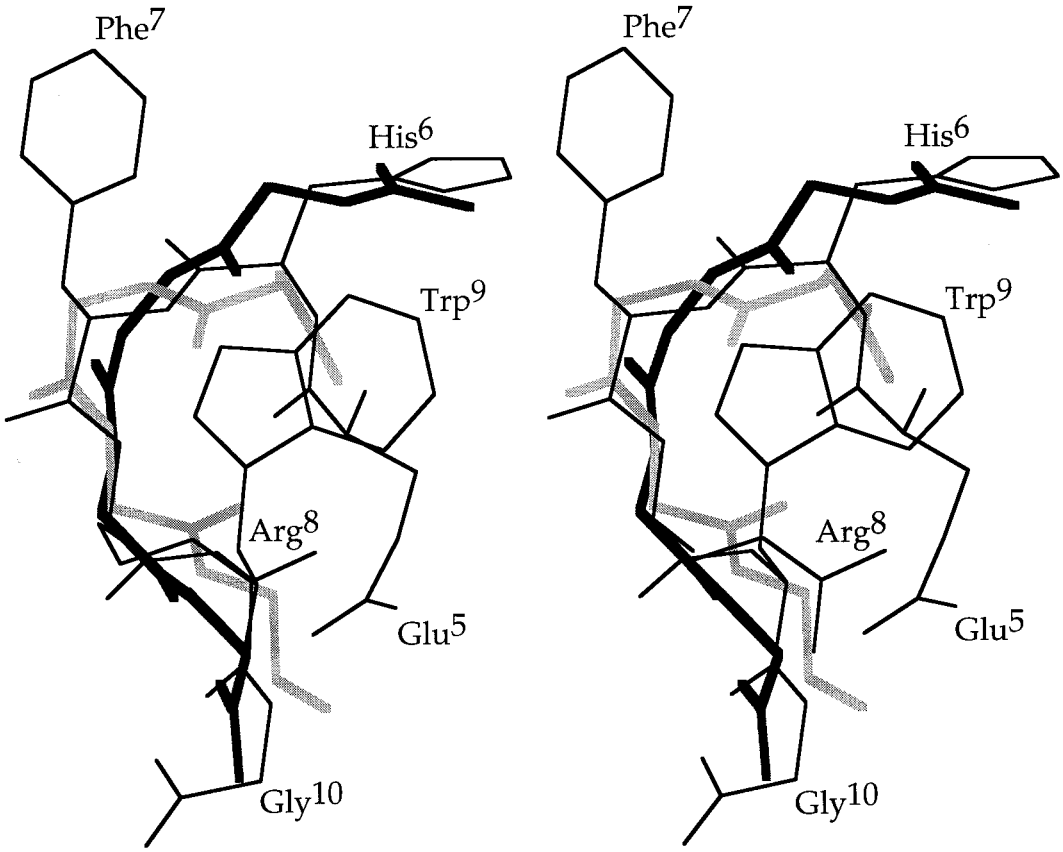

FIGURE 4 Overlapped stereoviews of various models of the biologically active conformer for [D-Phe^7]α-MSH: fragment 5–11, this study (thin black line); backbones of fragment 6–9 from Ref. 12 (thick black line, more extented) and Ref. 14 (thick shadow line). All hydrogens are omitted for clarity.

should be emphasized that these conformers are similar in terms of the mutual spatial arrangement of the His, Phe, Arg, and Trp sidechain moieties, rather than in terms of the similarity of their peptide backbone dihedral angle values. This is especially evident when comparing conformers in Table VI for active cyclic analogues and for linear α-MSH and [D-Phe^7]α-MSH peptides.

It is interesting to note that α-MSH conformer 1, listed in Table VI, is the same conformer that was suggested as a template for the biologically active conformation of α-MSH in our preliminary publication.[27] Conformer 14 of [D-Phe^7]α-MSH, which also is listed in Table IV, is close to the [D-Phe^7]α-MSH conformer of type I (see Table I in Ref. 27) providing the peptide bond planes between residues His-D-Phe, Arg-Trp, and Trp-Gly are rotated by ca. 180°.

Finally, it is worthwhile to compare the biologically active conformation of the backbone of the His-L/D-Phe-Arg-Trp message sequence proposed in this study, with those suggested by energy calculations earlier.[12,14] Figure 4 depicts the backbone in question for [D-Phe^7]α-MSH conformation (fragment 5–11) from this study (see Table VI) and from an earlier computational paper,[14] as well as from Sugg et al.[12] One can easily see a conformational similarity for both former structures, but only a modest resemblance to the other proposed[12] conformation, which has a loose chain reversal around the D-Phe^7-Arg^8 fragment. At the same time, the model for the bioactive conformation of Ac-[Nle^4, c[D-Orn^5, Glu^8)]α-MSH(4–11)-NH_2 revealed by nmr spectroscopy[15] is similar to that proposed in this study.

CONCLUSIONS

1. Energy calculations on α-MSH and [D-Phe^7]α-MSH were used to design cyclic peptides to stabilize different proposed conformational

isomers of the parent compounds. With minimal structural modifications of the conformationally flexible Gly^{10} residue (replacing of hydrogens by methyl groups), cyclic octa- and heptapeptide cyclic analogues with different conformational possibilities were designed. Some of these analogues showed biological potencies on frog skin comparable to the potencies of parent tridecapeptide.

2. Additional energy calculations for the obtained cyclic analogues allowed us to refine a model for the biologically active conformation of the His-Phe-Arg-Trp message sequence of α-MSH and [D-Phe^7]α-MSH. It was found that α-MSH and [D-Phe^7]α-MSH, as well as biologically potent cyclic analogues, possess similar low-energy conformations not in terms of close values for dihedral angles, but in terms of common spatial arrangements for functional groups involved in the ''message'' sequence.

This work was supported in part by U.S. Public Health Service grant DK17420.

REFERENCES

1. Eberle, A. (1988) *The Melanotropins: Chemistry, Physiology and Mechanism of Action*, S. Karger, Basel.
2. Cody, W. L., Stevenson, J. W. S., Al-Obeidi, F., Sugg, E. E. & Hruby, V. J. (1988) in *The Melanotropic Peptides*, Vol. III, Hadley, M. E., Ed., CRC Press, Boca Raton, FL, pp. 93–109.
3. Hruby, V. J., Wilkes, B. C., Cody, W. L., Sawyer, T. K. & Hadley, M. E. (1984) *Peptide Protein Rev.* **3,** 1–64.
4. Hruby, V. J., Wilkes, B. C., Hadley, M. E., Al-Obeidi, F., Sawyer, T. K., Staples, D. J., deVaux, A. E., Dym, O., Castrucci, A. M. d. L., Hintz, M. F., Riehm, J. P. & Rao, K. R. (1987) *J. Med. Chem.* **30,** 2126–2130.
5. Otsuka, H. & Inouye, K. (1964) *Bull. Chem. Soc. Jpn.* **37,** 289–290.
6. Eberle, A. & Schwyzer, R. (1975) *Helv. Chem. Acta* **58,** 1528–1535.
7. Eberle, A., Fauchere, J.-L., Tesser, G. I. & Schwyzer, R. (1975) *Helv. Chem. Acta* **58,** 2106–2129.
8. Sawyer, T. K., Sanfilippo, P. J., Hruby, V. J., Engel, M. H., Heward, C. B., Burnett, J. B. & Hadley, M. E. (1980) *Proc. Natl. Acad. Sci. USA* **77,** 5754–5758.
9. Sawyer, T. K., Hruby, V. J., Darman, P. S. & Hadley, M. E. (1982) *Proc. Natl. Acad. Sci. USA* **79,** 1751–1755.
10. Knittel, J. J., Sawyer, T. K., Hruby, V. J. & Hadley, M. E. (1983) *J. Med. Chem.* **28,** 125–129.
11. Cody, W. L., Mahoney, M., Knittel, J. J., Hruby, V. J., de L. Castrucci, A. M. & Hadley, M. E. (1985) *J. Med. Chem.* **28,** 583–588.
12. Sugg, E. E., Cody, W. L., Abdel-Malek, Z., Hadley, M. E. & Hruby, V. J. (1986) *Biopolymers* **25,** 2029–2042.
13. Nikiforovich, G. V., Shenderovich, M. D. & Chipens, G. I. (1981) *FEBS Lett.* **126,** 180–182.
14. Nikiforovich, G. V., Rozenblit, S. A., Shenderovich, M. D. & Chipens, G. I. (1984) *FEBS Lett.* **170,** 315–320.
15. Sugg, E. E., de L. Castrucci, A. M., Hadley, M. E., van Binst, G. & Hruby, V. J. (1988) *Biochemistry* **27,** 8181–8188.
16. Al-Obeidi, F., Hadley, M. E., Pettitt, B. M. & Hruby, V. J. (1989) *J. Am. Chem. Soc.* **111,** 3413–3416.
17. Al-Obeidi, F., Castrucci, A. M. L., Hadley, M. E. & Hruby, V. J. (1989) *J. Med. Chem.* **32,** 2555–2561.
18. Bodi, J., Medzihradszky-Schweiger, H. & Suli-Vargha, H. (1991) in *Peptides 1990, Proceedings of the 21st European Peptide Symposium*, Giralt, E. & and Andreu, D., Eds., ESCOM, Leiden, pp. 690–691.
19. Nikiforovich, G. V., Leonova, V. I., Galaktionov, S. G. & Chipens, G. I. (1979) *Int. J. Peptide Protein Res.* **13,** 363–373.
20. Nikiforovich, G. V., Hruby, V. J., Prakash, O. & Gehrig, C. A. (1991) *Biopolymers* **31,** 941–955.
21. *SYBYL 5.4 Theory Manual* (1991) Tripos Associates, St. Louis, MO.
22. Merrifield, R. B. (1963) *J. Am. Chem. Soc.* **86,** 304–308.
23. Castro, B., Dormoy, J. R., Evin, G. & Seive, C. (1973) *Tetrahed. Lett.* 1219–1222.
24. Shizume, K., Lerner, A. B. & Fitzpatrick, T. B. (1954) *Endocrinology* **54,** 553–560.
25. Huntington, T. & Hadley, M. E. (1974) *Endocrinology* **95,** 472–474.
26. Castrucci, A. M. L., Hadley, M. E. & Hruby, V. J. (1984) *Gen. Comp. Endocrinol.* **55,** 104–111.
27. Nikiforovich, G. V., Sharma, S. D., Hadley, M. E. & Hruby, V. J. (1992) in *Peptides: Chemistry and Biology. Proceedings of the Twelfth American Peptide Symposium*, Smith, J. A. & Rivier, J. E., Eds., ESCOM, Leiden, pp. 389–392.
28. Prasad, B. V. V. & Balaram, P. (1984) *CRC Crit. Rev. Biochem.* **16,** 307–348.
29. Wilkes, B., Hruby, V. J., Yamamura, H. I., Akiyama, K., de L. Castrucci, A. M., Hadley, M. E., Andrews, J. R. & Wan, Y. P. (1984) *Life Sci.* **34,** 977–984.